

SLNR-based User Scheduling in Multi-cell networks: from Multi-antenna to Large-Scale Antenna System

Yanchun Li¹, Guangxi Zhu¹, Hua Chen², Minh Jo³ and Yingzhuang Liu¹

¹Department of Electronics and Information Engineering, Huazhong University of Science and Technology, Wuhan, Hubei 430074 - China

[e-mail: yanchun, gxzhu, liuyz@hust.edu.cn]

²College of Mathematics and Computer Science, Wuhan Textile University, Wuhan, Hubei 430073 - China

[e-mail : 562054584@qq.com]

³Department of Computer and Information Science, Korea University, Sejong, - Korea

[e-mail: minhojo@korea.ac.kr]

*Corresponding author: Minh Jo and Hua Chen

Received October 29, 2013; revised December 10, 2013; accepted January 4, 2013; published February 9, 2014

Abstract

In this paper, we investigate the performance of Signal to Leakage and Noise Ratio (SLNR) based user scheduling in uplink of multi-cell with large-scale antenna system. Large antenna array is desired to improve the performance in future system by providing better beamforming capability. However, some studies have found that the signal channel is 'hardened' (becomes invariant) when the antenna number goes extremely large, which implies that the signal channel aware user scheduling may have no gain at all. With the mathematic tool of order statistics, we analyzed the signal and interference terms of SLNR in a homogeneous multicell network. The derived distribution function of signal and interference shows that the leakage channel's variance is much more influential than the signal channel's variance in large-scale antenna regime. So even though the signal channel is hardened, the SLNR-based scheduling can achieve remarkable multiuser diversity (MUD) gain due to the fluctuation of the uplink leakage channel. By providing the final SINR distribution, we verify that the SLNR-based scheduling can leverage MUD in a better way than the signal channel based scheduling. The Monte Carlo simulations show that the throughput gain of SLNR-based scheduling over signal channel based scheduling is significant.

Keywords: Large-scale antenna system, multi-cell, interference management, multiuser diversity

This research was supported by the National Research Foundation of Korea grant funded by the Korea government (MEST) (No. 2012-0004811), the Sino-Korea Joint Research Project under grant (No. 2012DFG12250) and Nature Science Fund of Hubei province under grant (No. 2013CFB309)

<http://dx.doi.org/10.3837/tiis.2014.03.013>

1. Introduction

User scheduling has been widely adopted in the uplink of MIMO multicell networks to improve system throughput. It can get significant multiuser diversity gain if the varying in channel is large and the channel state is known by scheduler. The latest engineering advances allow the multiple antennas to be extended to extremely large antenna array in a practical and affordable way [1]. This technology is named large-scale antenna system (a.k.a. massive MIMO). The large number of antennas is desired to improve the performance in future system by providing better signal capture capability. However, some studies have found that the signal channel is ‘hardened’ (becomes invariant) [2] when the antenna number goes extremely large. Moreover, the acquisition of channel state information (CSI) which is the prerequisite of scheduling becomes challenging since the channel size is large while the resources for channel training is limited. Thus, whether to schedule users or not in massive MIMO is a subject of particular interest. In this work, we investigate the performance of Signal to Leakage and Noise Ratio (SLNR)-based scheduling which is aware of the channel condition in both signal and leakage channels in large-scale antenna system.

Recent works show that accurate CSI is available in massive MIMO system, so the scheduling performance in high CSI accuracy regime is of particular interest. The pilot contamination was considered as a serious problem for massive MIMO [3]. The inaccurate CSI causes the hardening in both signal and interference channel so that the user scheduling gain vanishes. Recently, plenty of researches show that accurate CSI is acquirable for massive MIMO [4] [5] [6]. Thus, channel aware user scheduling is viable for massive MIMO system.

Moreover, we notice that, when the scheduled user in other cell is different from the user causes the pilot contamination, the precoding will be also un-correlated with the interfering channel. It also implies that the interference channel will not be hardened like the signal channel.

Motivated by knowing that the interference power fluctuates significantly, we consider deploying user scheduling to reduce the interference in multicell massive MIMO systems. The user scheduling schemes in [7] [8] exploit the users’ channel diversity on large-scale to implement cooperative downlink massive-MIMO transmission. Thus, the interference can be turned into signal. However, the exchanging of CSIs among cells faces numbers of challenges, e.g. delay, backhaul overhead (especially for very large antenna system). Thus, we are interested at the scheme which doesn’t need coordination among cells.

The SLNR-based scheduling can aware of the interference produced by local-cell user without assistance from other cells. It can suppress inter-cell interference opportunistically while boost signal [9]. The performance of SLNR-based scheduling has been studied in traditional multi-antenna system. In traditional multi-antenna system, the signal channel fluctuates much more significantly than interference channel. Our early study shows it can provide significant throughput gain [10]. However, in massive MIMO system, the channel hardening effect causes signal channel fluctuate less significantly. Whether the SLNR-based scheduling could still provide performance gain has not yet known.

In this work, we study the performance of user scheduling in high CSI accuracy regime. When the impact of interference on pilot is suppressed, the data receiving will be less affected by the mislead channel estimation. However, the interference on data becomes a non-negligible factor. Unlike the signal channel based scheduling scheme whose gain

vanishes in massive MIMO, we find that the SLNR-based scheduling can still provide profound performance gain even when the signal channel is hardened. The major contributions of this paper are as follows:

- 1) By the mathematic tool of *Order Statistics*, we analyzed the signal and interference terms in SLNR of a homogeneous multicell network. The way that signal is enhanced and interference is suppressed is illustrated.
- 2) We find that, for large-scale antenna system, the leakage channel's variance is much more influential than the signal channel's variance in large-scale antenna regime based on the derived distribution function of signal and interference. So, even though the signal channel is hardened, the SLNR-based scheduling can achieve remarkable multiuser diversity (MUD) gain due to the fluctuation of the leakage channel.
- 3) By providing the eventual SINR distribution, we verify that the SLNR-based scheduling can leverage MUD in a better way than the signal channel based scheduling. The Monte Carlo simulations show that the throughput gain of SLNR-based scheduling over signal channel based scheduling is significant.

This paper is organized as follows. Section 2 introduces the system model, describes MRC detector and uplink. Section 3 discusses the relationship between CSI accuracy and the fluctuation characteristics in effective signal and interference channels. After discovering the fluctuation in massive MIMO interference channel of multi-cell uplink, we provide a simple review of SLNR-based user scheduling, which can effectively exploit the channel fluctuation opportunistically, in Section 4. In Section 5, the distribution of scheduled user's SINR is derived. And the effect of multiuser diversity is interpreted. The Monte Carlo simulation results are presented in Section 6. And Section 7 concludes the paper.

We use following notations in the paper. $f_x(\cdot)$ and $F_x(\cdot)$ is the Probability Density Function (PDF) and Cumulative Distribution Function (CDF) of a Random Variable (RV), correspondingly.

2. System Model

We consider the uplink of a multi-cell system with M BSs. Denote the BS in cell m as B_m . BS is equipped with N_r antennas. Each BS serves K single-antenna users. The users are identified by their index in cell and cell index jointly, e.g. the k th user in cell m is denoted by $U_{m,k}$. The BS with multiple antennas can support more than one uplink data streams simultaneously. Due to the large antenna size, the inter-user interference is considered as being trivial for massive MIMO. Since we are particularly interested at intercell interference, we assume a BS serves one user on each uplink resource block for the sake of simplicity and tractability.

We consider the propagation channel with large-scale path loss and small-scale channel fading. Assume OFDM is deployed so that each subcarrier can be considered as flat fading. The large-scale pathloss power gain of the channel between BS B_m and the user $U_{n,k}$ is $\tau_{m,n,k}$, $1 \leq m, n \leq M$ and $1 \leq k \leq K$. For the signal channel between BS B_m and its user $U_{m,k}$, the small scale fading coefficient vector can be denoted by $\mathbf{h}_{m,k} \in \mathbb{C}^{N_r \times 1}$. For the interfering channel between BS B_m and any user from other cell, $U_{n,k}$, $m \neq n$, the small

scale fading coefficient vector can be denoted by $\mathbf{g}_{m,n,k} \in \mathbb{C}^{N_r \times 1}$. We assume independent Rayleigh fading for all channels, then the elements in $\mathbf{h}_{m,k}$ and $\mathbf{g}_{m,n,k(n)}$ follow i.i.d. complex Gaussian distribution $CN(0,1)$.

We assume that all BSs and users are perfectly synchronized and operate in Time Division Duplexing (TDD) mode with universal frequency reuse. So, the channel has downlink-uplink reciprocity after Tx-Rx hardwares are calibrated.

Denote the scheduled user of BS B_m as $k(m)$. The signal transmitted by the scheduled user of BS B_m is $x_{m,k(m)}$. All user send signal with uniform transmit power P^{UL} , so $E\left[|x_{m,k(m)}|^2\right] = P^{UL}$. The received signal at BS B_m is the superposition of the signal from the scheduled users in all cells,

$$\mathbf{y}_m = \mathbf{h}_{m,k(m)}\sqrt{\tau_{m,m,k(m)}}x_{m,k(m)} + \sum_{1 \leq n \leq M, n \neq m} \mathbf{g}_{m,n,k(n)}\sqrt{\tau_{m,n,k(n)}}x_{n,k(n)} + \mathbf{n}_m \quad (1)$$

where, the last term is the white Gaussian Noise at BS m , $\mathbf{n}_m \sim CN(0, P^{Noise} \mathbf{I}_{N_r})$.

We assume a simple single-user detector with linear filtering. All interference is treated as noise. Both the Maximal Ratio Combining (MRC) and the MMSE detector are commonly used in conventional MIMO systems. However, due to extremely large N_r , the matrix inversion operation in MMSE has high computational complexity. MRC receiver is considered here. For the signal of BS B_m 's scheduled user, the output of MRC receiver is

$$r_{m,k(m)} = \mathbf{v}_{m,k(m)}^H \mathbf{y}_m \quad (2)$$

where, $\mathbf{v}_{m,k(m)} = \hat{\mathbf{h}}_{m,k(m)} / \|\hat{\mathbf{h}}_{m,k(m)}\|$ is the normalized MRC receiving weight vector. $\hat{\mathbf{h}}_{m,k(m)}$ is the estimated channel vector.

Then, the uplink SINR of BS B_m can be represented by

$$\rho_{m,k(m)} = \frac{\tau_{m,m,k(m)} \left| \mathbf{v}_{m,k(m)}^H \mathbf{h}_{m,k(m)} \right|^2}{\sum_{1 \leq n \leq M, n \neq m} \tau_{m,n,k(n)} \left| \mathbf{v}_{m,k(m)}^H \mathbf{g}_{m,n,k(n)} \right|^2 + \sigma} \quad (3)$$

where, σ is the normalized noise power, $\sigma = P^{Noise} / P^{UL}$. Since both the signal and interference have been processed by vector $\mathbf{v}_{m,k(m)}$, we are interested at the effective channel that the signal and interference propagate through. $\mathbf{v}_{m,k(m)}^H \mathbf{h}_{m,k(m)}$ is effective channel for signal while $\mathbf{v}_{m,k(m)}^H \mathbf{g}_{m,n,k(n)}$ is the effective channel for interference. They jointly determines the achievable rate of this transmission, $\log_2(1 + \rho_m)$. The system performance can be evaluated by the average throughput per cell, $E\left[\log_2(1 + \rho_m)\right]$.

Here, we assume the duration of the channel measurement, feedback and the scheduled transmission is much less than the coherent time of the varying channel. So, the channel measurement/feedback overhead can be omitted. The channel can be seen as constant within a scheduling period.

3. Relation between CSI Accuracy and Signal/Interference Channel Characteristics

The CSI accuracy, and the coupling between user scheduling and pilot allocation, jointly determines the characteristics of effective signal and interference channel. In this section, we show that in different level of CSI accuracy, the effective signal and interference channel will present different level of fluctuation. Further, we find the opportunistic user scheduling can help decorrelating the precoding with interference channels, so that the interference channel has fluctuation independent of N_r .

To depict the CSI accuracy in multicell MIMO system with pilot contamination, we begin with examination of the fundamental channel estimation process. We assume MBS acquires channel state via uplink training according to the channel reciprocity in TDD mode. J orthogonal pilot sequences are reused among users. Denote the set of users using j th pilot sequence in cell m is $\Omega_{j,m}$. Assume each set has equal number of users, $|\Omega_{1,m}| = |\Omega_{2,m}| = \dots = |\Omega_{J,m}| = \frac{K}{J}$. For the case that the number of users in cell is larger than the number of pilot sequences ($K > J$), pilot sequences will be reused within a cell, $|\Omega_{j,m}| > 1$.

Due to the pilot reuse in interference channel, the estimated signal channel is contaminated by the interfering channels which use the same pilot sequences. In the most serious case, the estimated signal channel is the superposition of local signal channel and interference channel [5]. And in other cases, the pilot contamination is alleviated [4] [6]. The signal and interference channel can be seems as orthogonal to each other as N_r goes extremely large (from Lemma 1

in [5]), $\frac{\mathbf{h}_{m,k(m)}^H \mathbf{h}_{m,u}}{N_r}$, $\frac{\mathbf{h}_{m,k(m)}^H \mathbf{g}_{m,n,l}}{N_r}$ and $\frac{\mathbf{g}_{m,n,l}^H \mathbf{h}_{m,u}}{N_r} \rightarrow 0$. Thus, generally, the estimated signal

channel of user $U_{m,k(m)}$ can be expressed as

$$\hat{\mathbf{h}}_{m,k(m)} = \underbrace{\alpha_{m,k(m)} \mathbf{h}_{m,k(m)}}_{\text{signal channel}} + \underbrace{\sum_{u \in \Omega_{j,m} \setminus \{k(m)\}} \varphi_{(m,k(m)),(m,u)} \mathbf{h}_{m,u}}_{\text{intra-cell contamination}} + \underbrace{\sum_{1 \leq n \leq M} \sum_{l \in \Omega_{j,n}} \varphi_{(m,k(m)),(n,l)} \mathbf{g}_{m,n,l}}_{\text{intercell contamination}} + \mathbf{v}_{m,k(m)} \quad (4)$$

where, $\alpha_{m,k(m)}$, $\varphi_{(m,k(m)),(m,u)}$ and $\varphi_{(m,k(m)),(n,l)}$ are the scalar projection of $\hat{\mathbf{h}}_{m,k(m)}^H$ on $\mathbf{h}_{m,k(m)}$, $\mathbf{h}_{m,u}$ and $\mathbf{g}_{m,n,l}$, respectively. Since the vector $\mathbf{h}_{m,k(m)}$, $\mathbf{h}_{m,u}$ and $\mathbf{g}_{m,n,l}$ are not normalized, the above scalar projection of \mathbf{a} on \mathbf{b} shall be calculated by $\mathbf{a}^H \mathbf{b} / \|\mathbf{b}\|^2$. The coefficients $\alpha_{m,k(m)}$, $\varphi_{(m,k(m)),(m,u)}$ and $\varphi_{(m,k(m)),(n,l)}$ are determined by the performance of deployed pilot transmission design and channel estimation schemes jointly. $\mathbf{v}_{m,k(m)}$ is the residual part which can be calculated by

$$\mathbf{v}_{m,k(m)} = \hat{\mathbf{h}}_{m,k(m)} - \alpha_{m,k(m)} \mathbf{h}_{m,k(m)} - \sum_{u \in \Omega_{j,m} \setminus \{k(m)\}} \varphi_{(m,k(m)),(m,u)} \mathbf{h}_{m,u} - \sum_{1 \leq n \leq M} \sum_{l \in \Omega_{j,n}} \varphi_{(m,k(m)),(n,l)} \mathbf{g}_{m,n,l}$$

Note that when N_r is small, $\mathbf{h}_{m,k(m)}$, $\mathbf{h}_{m,u}$ and $\mathbf{g}_{m,n,l}$ are not strictly orthogonal with each

other, and that (4) is not a strict orthogonal decomposition of vector $\hat{\mathbf{h}}_{m,k(m)}$, so $\mathbf{v}_{m,k(m)}$ is weakly correlated with $\mathbf{h}_{m,k(m)}$, $\mathbf{h}_{m,u}$ and $\mathbf{g}_{m,n,l}$.

Then, we consider the data receiving with the estimated CSI. Combining (1) and (2), we can rewrite the received signal in form of

$$r_{m,k(m)} = \underbrace{\frac{\hat{\mathbf{h}}_{m,k(m)}^H \mathbf{h}_{m,k(m)}}{\|\hat{\mathbf{h}}_{m,k(m)}\|} \sqrt{\tau_{m,m,k(m)}} x_{m,k(m)}}_{\text{Signal}} + \underbrace{\sum_{1 \leq n \leq M, n \neq m} \frac{\hat{\mathbf{h}}_{m,k(m)}^H \mathbf{g}_{m,n,k(n)}}{\|\hat{\mathbf{h}}_{m,k(m)}\|} \sqrt{\tau_{m,n,k(n)}} x_{n,k(n)}}_{\text{Interference}} + \frac{\hat{\mathbf{h}}_{m,k(m)}^H \mathbf{n}_m}{\|\hat{\mathbf{h}}_{m,k(m)}\|} \quad (5)$$

First, we consider the signal term of above equation. From (4), we can know the component $\hat{\mathbf{h}}_{m,k(m)}^H \mathbf{h}_{m,k(m)}$ in the signal term has

$$\begin{aligned} \hat{\mathbf{h}}_{m,k(m)}^H \mathbf{h}_{m,k(m)} &= \alpha_{m,k(m)} \mathbf{h}_{m,k(m)}^H \mathbf{h}_{m,k(m)} + \sum_{u \in \Omega_{j,m} \setminus \{k(m)\}} \varphi_{(m,k(m)),(m,u)} \mathbf{h}_{m,u}^H \mathbf{h}_{m,k(m)} \\ &+ \sum_{1 \leq n \leq M} \sum_{l \in \Omega_{j,n}} \varphi_{(m,k(m)),(n,l)} \mathbf{g}_{m,n,l}^H \mathbf{h}_{m,k(m)} + \mathbf{v}_{m,k(m)}^H \mathbf{h}_{m,k(m)} \end{aligned} \quad (6)$$

$\mathbf{h}_{m,k(m)}$ is uncorrelated with $\mathbf{h}_{m,u}$ and $\mathbf{g}_{m,n,l}$. And residual term $\mathbf{v}_{m,k(m)}$ is neglectable. The pilot contamination's impact on the signal term can be evaluated by

$$\sigma_{m,k(m)}^2 = \sum_{u \in \Omega_{j,m} \setminus \{k(m)\}} \left| \varphi_{(m,k(m)),(m,u)} \right|^2 + \sum_{1 \leq n \leq M} \sum_{l \in \Omega_{j,n}} \left| \varphi_{(m,k(m)),(n,l)} \right|^2. \text{ If } \sigma_{m,k(m)}^2 \text{ is much larger than } \left| \alpha_{m,k(m)} \right|^2,$$

which means the pilot contamination is severe, the precoding vector $\mathbf{v}_{m,k(m)} = \hat{\mathbf{h}}_{m,k(m)} / \|\hat{\mathbf{h}}_{m,k(m)}\|$ can't match the signal channel $\mathbf{h}_{m,k(m)}$. In this case (CSI Accuracy level I in [Table 1](#)), the gain of effective signal channel will fluctuate. Despite fluctuation exists in level I, this case is not desirable at all due to the loss of multi-antenna beamforming gain. So, this case will be avoided in practical system. When the factor $\left| \alpha_{m,k(m)} \right|^2$ is significant, $\mathbf{h}_{m,k(m)}^H \mathbf{h}_{m,k(m)}$ is dominant in (6). So the signal channel becomes hardened when N_r goes larger (CSI Accuracy level II and III in [Table 1](#)).

Then, we consider the interference term in (5). The component $\hat{\mathbf{h}}_{m,k(m)}^H \mathbf{g}_{m,n,k(n)}$ in interference term has

$$\begin{aligned} \hat{\mathbf{h}}_{m,k(m)}^H \mathbf{g}_{m,n,k(n)} &= \alpha_{m,k(m)} \mathbf{h}_{m,k(m)}^H \mathbf{g}_{m,n,k(n)} + \sum_{u \in \Omega_{j,m} \setminus \{k(m)\}} \varphi_{(m,k(m)),(m,u)} \mathbf{h}_{m,u}^H \mathbf{g}_{m,n,k(n)} \\ &+ \sum_{1 \leq n \leq M} \sum_{l \in \Omega_{j,n}} \varphi_{(m,k(m)),(n,l)} \mathbf{g}_{m,n,l}^H \mathbf{g}_{m,n,k(n)} + \mathbf{v}_{m,k(m)}^H \mathbf{g}_{m,n,k(n)} \end{aligned}$$

Obviously, $\mathbf{h}_{m,u}^H, \forall u \neq k(m)$, is uncorrelated with $\mathbf{g}_{m,n,k(n)}$. So, the impact of intra-cell pilot contamination can be neglected.

When the characteristics which exist in realistic propagation channels are not exploited at all, the signal channel and interference channel are indistinguishable [\[5\]](#). In such case,

$|\alpha_{m,k(m)}|^2$ and $\sigma_{m,k(m)}^2$ are comparable and the pilot contamination is serious. The work in [5] assumes all users reusing the same pilot sequence are scheduled simultaneously. The term $\mathbf{g}_{m,n,k(n)}$ in $\hat{\mathbf{h}}_{m,k(m)}$ causes the hardening in interference channel (CSI accuracy level II in Table 1). Obviously, there is also hardening in interference channel for the CSI accuracy level I.

Table 1. Relation between CSI Accuracy and Signal/Interference Channel Characteristics in massive MIMO System

CSI Accuracy Level	Parameters in estimated channels	Effective Signal Channel	Effective Interference Channel
I	$ \alpha_{m,k(m)} ^2 \ll \sigma_{m,k(m)}^2$	Fluctuating	Hardened
II	$ \alpha_{m,k(m)} ^2$ and $\sigma_{m,k(m)}^2$ are comparable	Hardened	Hardened
III	$ \alpha_{m,k(m)} ^2 \rightarrow 1, \sigma_{m,k(m)}^2 \rightarrow 0$	Hardened	Fluctuating

Recent works show that, by exploiting the channel statistical feature in realistic environment, the sophisticated pilot sequence assignment [4] and pilot stage allocation scheme [5] can estimate the signal channel quite accurately. The simulation in shows that the mean square error of the estimation, $tr\left(E\left[\left(\hat{\mathbf{h}}_{m,k(m)} - \mathbf{h}_{m,k(m)}\right)\left(\hat{\mathbf{h}}_{m,k(m)} - \mathbf{h}_{m,k(m)}\right)^H\right]\right)$, can be extremely small and the estimation result even approaches the interference-free case. We denote it as the accuracy level III in Table 1. A pilot sequence allocation scheme has been proposed in [4] which shows that the contamination factor is small and α approaches 1 ($\sigma_{m,k(m)}^2 \rightarrow 0$, correspondingly). In this CSI accuracy level, the correlation between $\hat{\mathbf{h}}_{m,k(m)}$ and $\mathbf{g}_{m,n,k(n)}$ is small and the interference channel become fluctuating.

Moreover, we find that the interference channels are no longer hardened when multi-user scheduling is deployed. Assuming the scheduled user in cell m using the j th pilot sequence, $k(m) \in \Omega_{j,m}$ and all user has equal scheduling oppurtunities. The pilot contamination is most damaging when $k(n) \in \Omega_{j,n}$ as in [5]. The receiving vector will partial match the direction where the interference comes from. In fact, the probability of this event is small, $P\{k(n) \in \Omega_{j,n}\} = |\Omega_{j,n}|/K = J^{-1}$. The case that the user using other pilot sequence in cell n is more probable, $P\{k(n) \notin \Omega_{j,n}\} = (K - |\Omega_{j,n}|)/K = 1 - J^{-1}$. The interfering channel $\mathbf{g}_{m,n,l}$ from cell n is uncorrelated with the channel which causes the pilot contamination $\mathbf{g}_{m,n,k(n)}$. So the interference channels are no longer hardened when N_r goes larger.

The scheduling performance in CSI accuracy level III has not yet been studied by any existing papers. In later of this work, we consider the CSI accuracy level III and exploit the channel characteristics to achieve throughput gain.

4. Exploiting Channel Fluctuation in MIMO Multi-cell System

In this section, we study how SLNR-based scheduling helps boosting the SINR in multicell system. Since the SLNR-based user scheduling in uplink affects the SINR distribution in indirect way, to obtain of distribution of the resulting SINR, we shall first know the distributions of scheduled user's signal and interference which are associated with the maximal SLNR. And these distributions rely on the distribution of maximal SLNR which is affected by the number of candidate users. So we derive the distribution of the scheduled user's SLNR, signal, interference and SINR, one by one.

The SLNR-based scheduler has the benefit of exploiting the fluctuation in both signal and interference channels [10]. The SLNR of user $U_{m,k}$ is

$$\lambda_{m,k} = \frac{\tau_{m,m,k} \left| \mathbf{v}_{m,k}^H \mathbf{h}_{m,k} \right|^2}{\sigma + \sum_{1 \leq n \leq M, n \neq m} \tau_{n,m,k} \left| \mathbf{v}_{n,k(n)}^H \mathbf{g}_{n,m,k} \right|^2}. \quad (7)$$

The SLNR aware scheduler can pick the user with highest SLNR,

$$k(m) = \arg \max_{1 \leq k \leq K} \lambda_{m,k}. \quad (8)$$

The SLNR-based scheduling gain relies on the small scale channel fluctuation in (7). To simplify the notation and ease the analysis, we define the small-scale power gain of effective channel for both signal and interference channel. The small-scale power gain of effective signal channel of user $U_{m,k}$ is $s_{m,k} = \left| \mathbf{v}_{m,k}^H \mathbf{h}_{m,k} \right|^2 \sim \chi^2(2N_r)$, where $\chi^2(2N_r)$ stands for the chi-squared distribution with $2N_r$ degrees of freedom. The small-scale power gain of the effective leakage channel between user $U_{m,k}$ and a BS interfered by it, B_n , $n \neq m$, is $q_{n,m,k} = \left| \mathbf{v}_{n,k}^H \mathbf{g}_{n,m,k} \right|^2 \sim \chi^2(2)$. For the sake of tractability, we assume a homogeneous large-scale channel model in all cells. We consider the same pathloss for all users' signal channels, $\tau_{m,m,k} = g_s$, $1 \leq m \leq M$, $1 \leq k \leq K$. Similarly, the pathloss gains in all interfering channels are also the same, $\tau_{n,m,k} = g_p$, $\forall n \neq m$.

In uplink, the aggregated leakage produced by user $U_{m,k}$ to all BSs interfered by it is

$$p_{m,k} = \sum_{n \neq m} q_{n,m,k} \sim \chi^2(2M - 2). \quad (9)$$

So, the SINR in (7) can be rewritten as $\lambda_{m,k} = \frac{g_s s_{m,k}}{\sigma + g_p p_{m,k}}$.

4.1 The Impact of Scheduling on SLNR

First, we consider the distribution of RVs before scheduling, which is call pre-scheduling distribution. The signal and pollution's channel distributions, $f_{s_{n,m}}(s)$ and $f_{p_{n,m}}(p)$, jointly determine the distribution of pre-scheduling SLNR. For any user $U_{m,k}$, it has pre-scheduling SLNR $\lambda_{m,k}$ which has PDF of

$$f_{\lambda_{m,k}}(\lambda) = \int_0^\infty \left(\frac{ds_{m,k}}{d\lambda_{m,k}} \right) f_{s_{m,k}}(s) \Big|_{s=\frac{\lambda(\sigma+g_P p)}{g_S}} \cdot f_{p_{m,k}}(p) dp \quad (10)$$

By taking $s = \frac{\lambda(\sigma + g_P p)}{g_S}$, and the assumed PDF of $s_{n,m}$ and $p_{n,m}$ into (10), we can get

$$f_{\lambda_{m,k}}(\lambda) = \frac{\lambda^{N_r-1}}{(N_r)! g_S^{N_r} (M-2)!} \int_0^\infty (\sigma + g_P p)^{N_r} e^{-\frac{\lambda\sigma}{g_S} \left(\frac{\lambda g_P + 1}{g_S} \right) p} p^{M-2} dp. \quad (11)$$

Further, by expanding the term $(\sigma + g_P p)^{N_r}$, we can get

$$f_{\lambda_{m,k}}(\lambda) = \frac{\lambda^{N_r-1}}{(N_r)! g_S^{N_r} (M-2)!} \int_0^\infty \sum_{i=0}^{N_r} \frac{(N_r)!}{(N_r-i)!(i)!} \sigma^{N_r-i} (g_P p)^i e^{-\frac{\lambda\sigma}{g_S} \left(\frac{\lambda g_P + 1}{g_S} \right) p} p^{M-2} dp. \quad (12)$$

The Eq. (12) can be rewritten as

$$f_{\lambda_{m,k}}(\lambda) = \frac{\lambda^{N_r-1} e^{-\frac{\lambda\sigma}{g_S}}}{(N_r)! g_S^{N_r} (M-2)!} \sum_{i=0}^{N_r} \left(\frac{(N_r)!}{(N_r-i)!(i)!} \sigma^{N_r-i} g_P^i \left(\frac{\lambda g_P}{g_S} + 1 \right)^{1-M-i} \int_0^\infty e^{-\left(\frac{\lambda g_P + 1}{g_S} \right) p} \left(\left(\frac{\lambda g_P}{g_S} + 1 \right) p \right)^{M+i-2} \left(\frac{\lambda g_P}{g_S} + 1 \right) dp \right). \quad (13)$$

Finally, by applying $\int_0^\infty e^{-z} z^{M-1} dz = (M-1)!$ to (13), we can get the exact form of $\lambda_{m,k}$'s PDF

$$f_{\lambda_{m,k}}(\lambda_{m,k}) = \frac{\lambda^{N_r-1} e^{-\frac{\lambda\sigma}{g_S}}}{(N_r)! g_S^{N_r} (M-2)!} \sum_{i=0}^{N_r} \left(\frac{(N_r)!}{(N_r-i)!(i)!} \sigma^{N_r-i} g_P^i \left(\frac{\lambda g_P}{g_S} + 1 \right)^{1-M-i} (M+i-2)! \right) \quad (14)$$

Thus, the CDF of $\lambda_{m,k}$ can be derived as

$$F_{\lambda_{m,k}}(\lambda) = \int_0^\lambda f_{\lambda_{m,k}}(x) dx = \frac{1}{(N_r)! g_S^{N_r} (M-2)!} \sum_{i=0}^{N_r} \left(\frac{(N_r)!}{(N_r-i)!(i)!} \sigma^{N_r-i} g_P^i (M+i-2)! \theta(i) \right) \quad (15)$$

where, $\theta(i) = \sum_{j=0}^{1-M-i} \frac{(1-M-i)!}{(1-M-i-j)!(j)!} \frac{g_P^j}{g_S^j} \left(\frac{\sigma}{g_S} \right)^{-N_r-j} \gamma \left(N_r + j, \frac{\sigma}{g_S} \lambda_{n,m} \right)$

For the special case that $N_r = 1$, it has simple closed form

$$F_{\lambda_{m,k}}(\lambda) = 1 - e^{-\frac{\lambda n}{g_S} \left(\frac{\lambda g_P}{g_S} + 1 \right)^{1-M}}$$

Based on the distribution of pre-scheduling RVs and the behavior of scheduling, the

distribution of the post-scheduling RVs can be obtained. We consider the impact of user scheduling. The event that the maximal SLNR in cell m has value of λ is equivalent to the event that any other users in cell have SLNRs smaller than λ ,

$$P\{\lambda_{m,k(m)} = \lambda\} = P\{\lambda_{m,k} \leq \lambda, \forall k \neq k(m)\}.$$

Besides, this user $k(m)$ can be any one of K users. So, by order statistics [11], the PDF of the scheduled user's SLNR can be derived as

$$f_{\lambda_{m,k(m)}}(\lambda) = f_{\lambda_{m,k}}(\lambda) \cdot K \left(F_{\lambda_{m,k}}(\lambda) \right)^{K-1}$$

And the CDF of $\lambda_{m,k(m)}$ is

$$F_{\lambda_{m,k(m)}}(\lambda) = \left(F_{\lambda_{m,k}}(\lambda) \right)^K \tag{16}$$

The CDFs of scheduled users' SLNR, calculated by (16) for the cases of $M = 4$, $K = 10$ and $N_r = 1, 16, 256$ is shown in Fig.1. The variance of SLNR becomes smaller with the increase of BS's antenna number. It can be interpreted by the hardening of signal channel at large N_r . Considering the performance of median user, the post-scheduling SLNR has 2.9dB gain over the pre-scheduling SLNR.

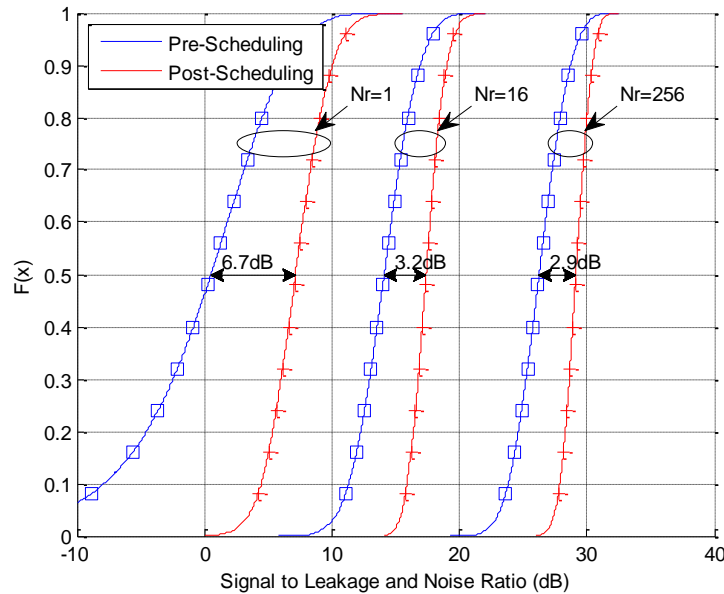


Fig. 1. The CDF of pre- and post-scheduling SLNRs with various antenna configurations for $g_S / g_P = 3dB$ and $g_P / \sigma = 5dB$. The theoretical results are shown by solid lines, while the Monte Carlo results of Pre-Scheduling and Post-Scheduling are presented by the markers \square and $+$, respectively. The markers are all coincident with their corresponding lines.

4.2 Analysis of Scheduling's Effect on Signal Enhancement and Interference Suppression

Since the $\lambda_{m,k(m)}$ is the largest among all K users' SLNRs, the signal term in it, $s_{m,k(m)}$, tends

to be large while the pollution term, $q_{n,m,k}$, tends to be small.

First, we consider the distribution of signal term, $s_{m,k(m)}$. The signal channel power gain of the selected user $s_{m,k(m)}$ is associated with the SLNR $\lambda_{m,k(m)}$ greater than the other $K-1$ users. So the $s_{m,k(m)}$'s PDF is

$$f_{s_{m,k(m)}}(s) = \int_0^{\infty} K \cdot F_{\lambda_{m,k}}^{K-1}(\lambda) \Big|_{\lambda = \frac{g_s s}{\sigma + g_p p}} \cdot f_{s_{m,k}}(s) f_{p_{m,k}}(p) dp \quad (17)$$

In (17), the multiplier K comes from $\binom{1}{K}$ which means that any user could be the one with highest SLNR. When $p_{m,k}$ traverses over the range $(0, +\infty)$, the value of $\lambda_{m,k(m)}$ is adjusted to $\lambda = \frac{g_s s}{\sigma + g_p p}$, accordingly. $F_{\lambda_{m,k}}^{K-1}(\lambda)$ is the probability that all users other than $k(m)$ in cell m have SLNR smaller than λ .

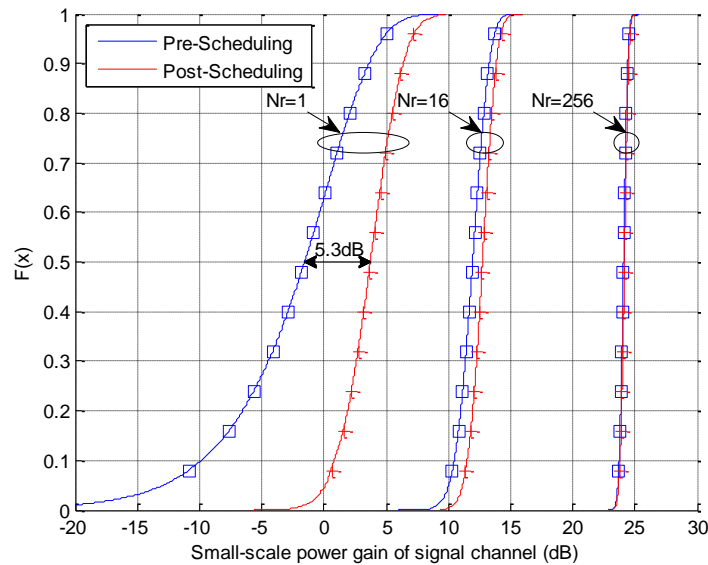


Fig. 2. The CDF of effective signal power gain in small-scale channel fading. The theoretical results are shown by solid lines, while the Monte Carlo results of Pre-Scheduling and Post-Scheduling are presented by the markers \square and $+$, respectively.

Unfortunately, there's no closed form expression for the integral result in (17). By taking (14) and (15) into (17), $s_{m,k(m)}$'s PDF can be calculated by numerical method. The CDFs of scheduled users' signal channel power gain $s_{m,k(m)}$ and all users' signal channel power gain $s_{m,k}$ ($1 \leq k \leq K$) are presented in **Fig.2**. When N_r is small, $s_{m,k}$ has significant fluctuation. The scheduler can easily exploit the channel diversity to enhance the signal channel power gain of scheduled users. However, when N_r goes large, the hardening effect of massive

MIMO's signal channel emerges. For $N_r = 256$, the varying of $s_{m,k}$ is so small that SLNR-based scheduler could hardly pick any user with higher $s_{m,k}$.

While the higher SLNR tends to be associated with a higher signal channel gain $s_{m,k}$, it also pursues a lower leakage channel gain $q_{n,m,k}$. However, the situation for $q_{n,m,k(m)}$ is more complicate than for $s_{m,k(m)}$, since in $\lambda_{m,k(m)}$, the channel power gains of leakage to several BSs are summed, $p_{m,k} = \sum_{n \neq m} q_{n,m,k}$.

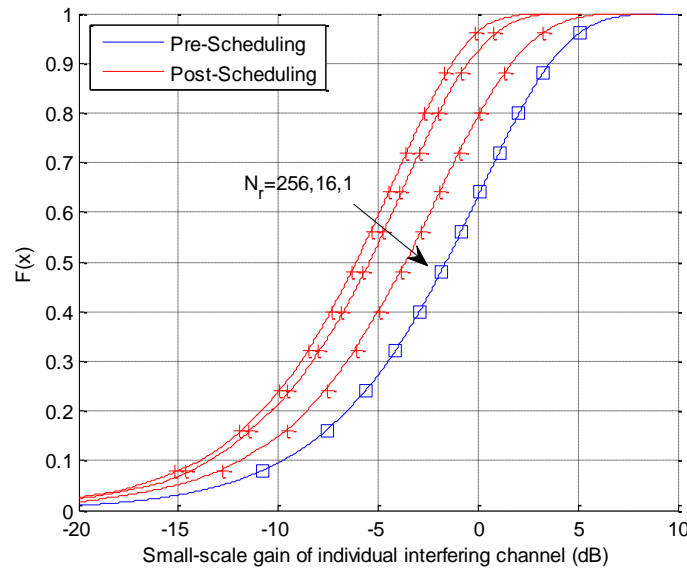


Fig. 3. Distribution of individual interference channel's small scale gain $q_{n,m,k}$, $\forall n \neq m$, under various antenna configurations. The theoretical results are shown by solid lines, while the Monte Carlo results of Pre-Scheduling and Post-Scheduling are presented by the markers \square and $+$, respectively.

First, we consider the aggregated pollution by the user k in cell m to all interfered BSs except a interfered BS $i \neq m$, which is denoted as $\bar{p}_{\neq i,m,k}$,

$$\bar{p}_{\neq i,m,k} = \sum_{j \neq m,i} q_{j,m,k} \sim \chi^2(2M - 4).$$

The PDF of $\bar{p}_{\neq i,m,k}$ is

$$f_{\bar{p}_{\neq i,m,k}}(\bar{p}) = \frac{1}{(M - 3)!} \bar{p}^{M-3} e^{-\bar{p}} \tag{18}$$

Obviously, from the definition in (9), we can know

$$p_{m,k} = q_{i,m,k} + \bar{p}_{\neq i,m,k} \tag{19}$$

By (18) and (19), we can get

$$f_{q_{i,m,k(m)}}(q) = f_{q_{i,m,k}}(q) \cdot \int_0^\infty f_{s_{m,k}}(s) \cdot \int_0^\infty K \cdot F_{\lambda_{m,k}}^{K-1}(\lambda) \Big|_{\lambda = \frac{g_s s}{\sigma + g_p q + g_p \bar{p}}} f_{\bar{p}_{\neq i,m,k}}(\bar{p}) d\bar{p} ds \tag{20}$$

There is no closed form expression for the scheduled pollution channel power gain's

expression either. We calculate (20) by numerical integration. The CDF of individual interference channel's small-scale gain at BS is shown in Fig.3. The distribution of pre-scheduling interference channel gain $q_{n,m,k}$ is independent of N_r . After scheduling, the interference channel gain is suppressed effectively. And the suppression is more significant when N_r is large. It is because that when signal channel is hardened at large antenna number regime, the fluctuation in SLNR is dominated by the varying in pollution channel.

Denote the aggregate interference in uplink data SINR (3) as

$$\omega_{m,k(m)} = \sum_{1 \leq n \leq M, n \neq m} \tau_{m,n,k(n)} q_{m,n,k(n)}.$$

We can get its CDF based on (20),

$$F_{\omega_{m,k(m)}}(\omega) = \iiint_{q_1 + q_2 + \dots + q_{M-1} \leq \omega} f_{q_{i,m,k(m)}}(q_1) f_{q_{i,m,k(m)}}(q_2) \dots f_{q_{i,m,k(m)}}(q_{M-1}) dq_1 dq_2 \dots dq_{M-1}$$

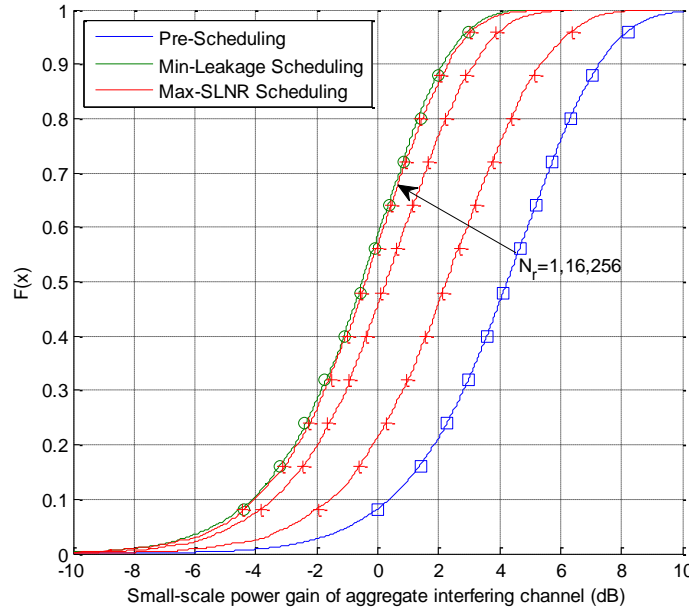


Fig. 4. Aggregate interfering channels' small-scale gain under various antenna configurations ($N_r = 1, 16, 256$). The theoretical results are shown by solid lines, while the Monte Carlo results of Pre-Scheduling, Min-Leakage Scheduling and Max-SLNR Scheduling are presented by the markers \square , \circ and $+$, respectively.

The consequent aggregate interference channel gain's distributions are shown in Fig.4. The most left CDF curve (green) is from *min-leakage scheduling* scheme, $k(m) = \arg \max_{1 \leq k \leq K} p_{m,k}$.

We compare the result of max-SLNR scheduling with it. At $N_r = 256$, the $\omega_{m,k(m)}$'s CDF curve under max-SLNR scheduling is almost aligned with the curve under min-leakage scheduling. It is because that the signal channel becomes hardened as shown in Fig.2. The fluctuation in $\lambda_{m,k}$ is primarily contributed by the variance of $q_{n,m,k}$. So, in large antenna regime, max-SLNR scheduler behaves similar to min-Leakage scheduler.

Note that we consider the interference is much more significant than noise. Although in

energy efficient (“green”) regime, the BS’s transmit power for massive MIMO may be low enough that the inter-cell interference is drowned in thermal noise, the achievable rate for each spatial stream is also low. To achieve extreme high data rate and satisfy user’s application demand, the per-stream rate must be high since the supportable spatial stream number at each user is limited. Thus, high-order modulations are used. The interference will be significantly above the noise level.

We can conclude that

- 1) The SLNR-based scheduling exploits the fluctuations in signal and interference channel.
- 2) It always tends to find a user with larger signal channel power gain and smaller leakage channel power gain among all users in a BS. And the preference is adapted to the variances in signal and leakage channels.

4.3 The impact of Scheduling on SINR

The SINR’s PDF can be derived in similar way of obtaining $f_{\lambda_{m,k}}(\lambda)$,

$$f_{\rho_{m,k(m)}}(\rho) = \int_0^{\infty} \left(\frac{ds_{m,k}}{d\rho_{m,k(m)}} \right) f_{S_{m,k(m)}}(s) \Big|_{s=\frac{\rho(\sigma+g_p\omega)}{g_s}} \cdot f_{\omega_{m,k(m)}}(\omega) d\omega.$$

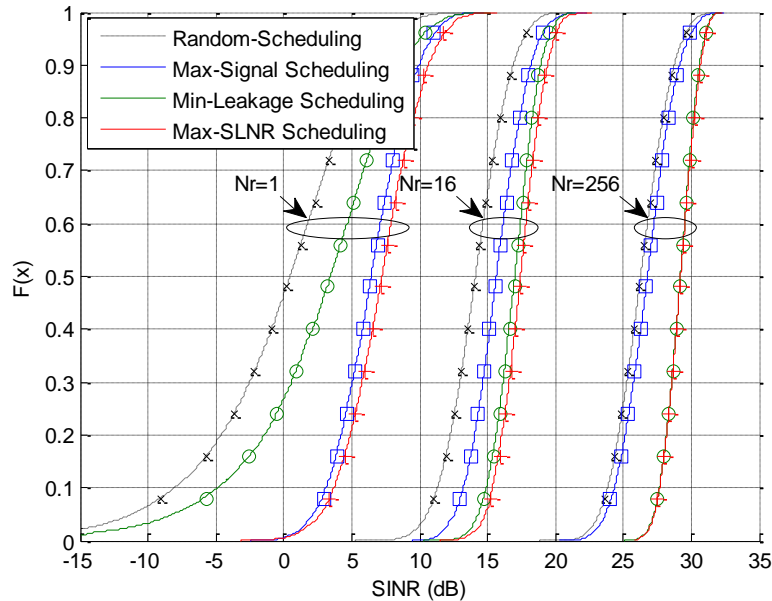


Fig. 5. SINR distribution under various antenna configurations. The theoretical results are shown by solid lines, while Monte Carlo results of Random Scheduling, Max-Signal Scheduling, Min-Leakage Scheduling and Max-SLNR Scheduling are presented by the markers \times , \square , \circ and $+$, respectively.

The average per-cell capacity in system is

$$C = \frac{1}{M} \sum_{1 \leq m \leq M} E \left\{ \log_2 \left(1 + \rho_{m,k(m)} \right) \right\} = \int_0^{\infty} \log_2 (1 + \rho) \cdot f_{\rho_{m,k(m)}}(\rho) d\rho$$

The final SINRs’ CDF under various scheme and different antenna configurations is shown in **Fig. 5**. By opportunistically selecting the user with high SPR, the spectrum efficiency of all

users is increased, especially in high spectrum efficiency region. The SLNR based scheduling's SINR is always beyond the SINR under max-Signal scheme and min-Leakage scheme.

From the analysis above, we conclude the main differences between the SLNR-based scheduling in traditional MIMO and Massive MIMO in **Table 2**.

Table 2. Comparison of SLNR based scheduling in massive MIMO and traditional MIMO

	Traditional MIMO	Massive MIMO
Effective Signal Channel	Fluctuating	Hardened
Effective Interference Channel	Fluctuating	Fluctuating
SLNR	Fluctuating	Less Fluctuating
Post-Scheduling SINR	Significantly improvement contributed by the fluctuation in both signal and interfering channels	Improvement mainly contributed by the fluctuation in interfering channels

5. Simulation Results

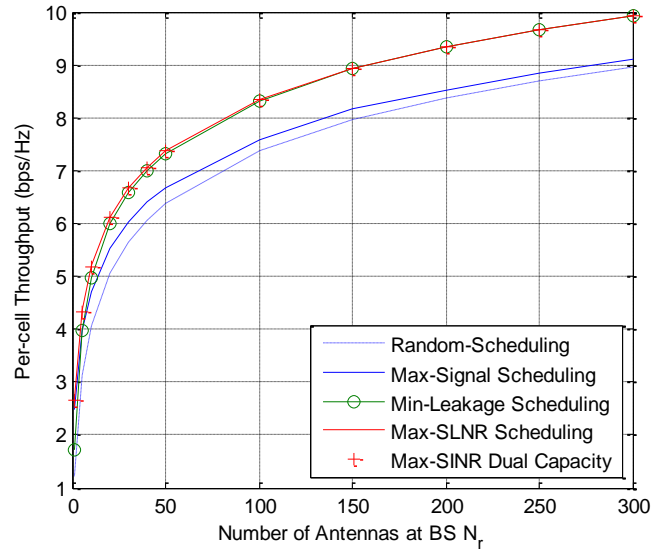
We compare the performance of various schemes by Monte Carlo simulations. Unless specified otherwise, we assume the per-cell user number is $K = 10$. And the major interfered BS number $M - 1$ is 3. The total BS number is $M = 4$. The large scale signal to interference power ratio is $g_S / (M - 1) g_P = 3dB$. The large scale interference to noise ratio is $(M - 1) g_P / \sigma = 5dB$.

The average per-cell throughputs with increasing BS antenna number is show in **Fig. 6**. It shows that the max-SLNR scheduling scheme has the highest throughput for all BS antenna configurations. We provide **Fig. 6(b)** to give a detailed view of the throughputs in low antenna number cases. Initially, when BS antenna number is small, the max-SLNR scheduling scheme achieves 1.87 times throughput of the random scheduling scheme. And the gain of max-signal scheduling over random user selection is also significant. By recalling the result from Section 4.2, we can find that the variance in signal channel is much larger than the variance in interference (leakage) channel, so the max-signal can achieve almost the same performance as max-SLNR scheme.

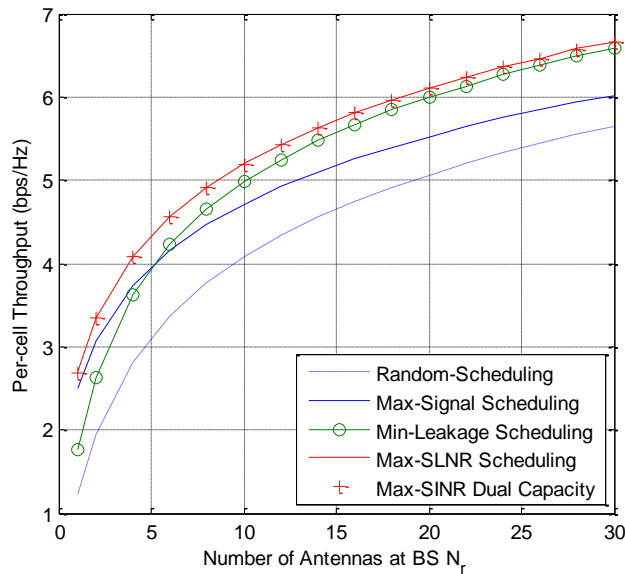
When BS antenna number becomes extremely large ($N_r = 128$), the gain of max-signal scheduling over random user selection vanishes. It can be interpreted as that users' signal channels are hardened with increasing antenna number.

Comparing to the performance gap between max-signal scheduling and random scheduling at $N_r = 128$, the performance gain of max-SLNR scheduling over max-signal scheduling is preminent. It is because that the fluctuation in leakage channel does not vanish with the increasing of BS antenna number. The varying in leakage channel becomes dominant when the signal channel power gain is almost fixed.

It is worth noting that the MUD gain from signal channel is so limited while the cost of acquiring signal channel state increases linearly with N_r [12]. This cost may outweigh the MUD gain benefit within it when $N_r \rightarrow \infty$. However, the cost of acquiring effective leakage channel does not increase with N_r . The throughput of min-Leakage scheduling is very approaching the throughput of max-SLNR scheduling. It suggests that the gain of MUD in leakage channel is dominant in large-scale antenna regime.



(a) Large-scale antenna number regime



(b) Small-scale antenna number regime

Fig. 6. The throughputs in various schemes with increasing antenna number

We evaluate the throughput achieved by various scheduling schemes with increasing per-cell user number K . To show how throughput is improved with K , we use the dual capacity of uplink MAC channels, the sum rate of the downlink broadcast channel, as the baseline. It is well known that, the per-cell sum-rate of the *max-SINR scheduling* in downlink demonstrates the growth rate of $\log \log K$, asymptotically with increasing number of users per-cell K [13]. From Fig. 7 we can see that the $\log \log K$ like MUD gain is also achievable in multicell uplink. The achievable rate of $\log \log K$ like has been found in early work [14]. It adopts a leakage-threshold based pre-qualifying stage to preclude the user who may cause

strong leakage to be the candidate. Then, the user with best signal channel is scheduled. However, it is hard to be applied to the multicell uplink with large-scale antenna because of the signal channel hardening. In contrast with it, SLNR based scheme can adapt to the varying of fluctuation characteristics in channels smoothly.

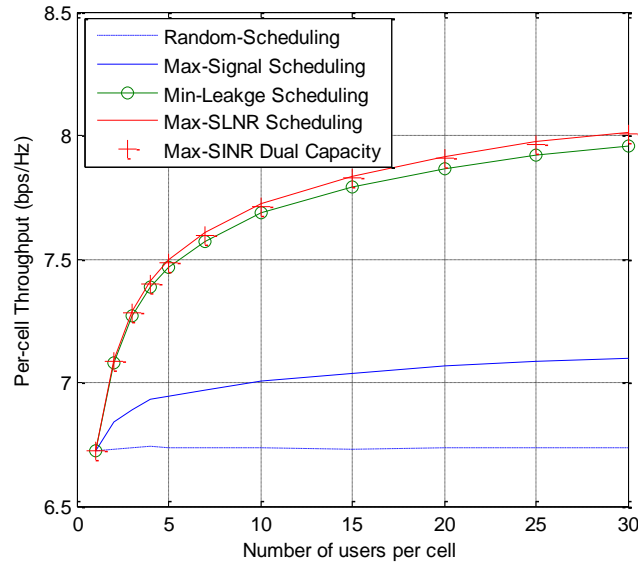


Fig. 7. Per-cell Throughput vs. User Number

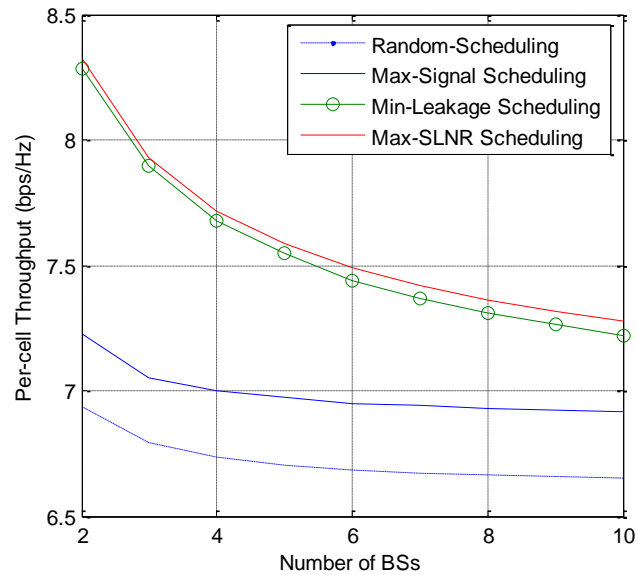


Fig. 8. Per-cell Throughput vs. BS Number M

Fig. 8 shows the impact of BS number's impact on throughputs. We can see that all scheduling schemes' per-cell throughputs decrease with the increasing of M . It is because that the aggregated leakage tends to be less fluctuating when M is large, as we can see from (9). Its impact on leakage-aware schemes including our SLNR-based scheduling is significant when $M = 10$. However, in practical networks, the number of BSs that cause strong

interference to local cell is small. For all cases of $M = 2, 3$ and 4, the performance gains of SLNR-based scheduling compared with Max-Signal scheduling are over 10%.

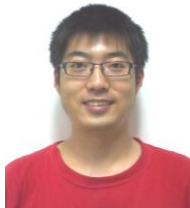
6. Conclusion

In this work, we investigate the performance of the SLNR-based user scheduling in uplink of multi-cell with large-scale antenna system. We find that in high CSI accuracy regime, with awareness of not only signal power but also the leakage power, the SLNR-based scheduling can try best efforts to suppress users' interference power leakage to other cells' BS when the signal channel is hardened in massive MIMO regime. So, generally, the SLNR-base scheduling can provide excellent performance in all antenna number configurations. With the mathematic tool of Order Statistics, we analyzed the signal and interference terms in SLNR of a homogeneous multi-cell network. The derived distribution function of signal and interference shows that the leakage channel's variance is much more influential than the signal channel's variance in large-scale antenna regime. So, the SLNR-based scheduling can leverage MUD in a better way than the scheduling schemes which only focus on signal channels. The Monte Carlo simulations show that the throughput gain of SLNR-based scheduler over signal channel based one is significant.

References

- [1] F. Rusek, D. Persson, L. Buon Kiong, E. G. Larsson, T. L. Marzetta, O. Edfors, and F. Tufvesson, "Scaling Up MIMO: Opportunities and Challenges with Very Large Arrays," *Signal Processing Magazine, IEEE*, vol. 30, pp. 40-60, 2013. [Article \(CrossRef Link\)](#).
- [2] B. M. Hochwald, T. L. Marzetta, and V. Tarokh, "Multiple-antenna channel hardening and its implications for rate feedback and scheduling," *Information Theory, IEEE Transactions on*, vol. 50, pp. 1893-1909, 2004. [Article \(CrossRef Link\)](#).
- [3] J. Hoydis, S. ten Brink, and M. Debbah, "Massive MIMO in the UL/DL of Cellular Networks: How Many Antennas Do We Need?," *Selected Areas in Communications, IEEE Journal on*, vol. 31, pp. 160-171, 2013. [Article \(CrossRef Link\)](#).
- [4] H. Yin, G. D., F. M., and Y. Liu, "A Coordinated Approach to Channel Estimation in Large-Scale Multiple-Antenna Systems," *Selected Areas in Communications, IEEE Journal on*, vol. 31, pp. 264-273, 2013. [Article \(CrossRef Link\)](#).
- [5] F. Fernandes, A. Ashikhmin, and T. L. Marzetta, "Inter-Cell Interference in Noncooperative TDD Large Scale Antenna Systems," *Selected Areas in Communications, IEEE Journal on*, vol. 31, pp. 192-201, 2013. [Article \(CrossRef Link\)](#).
- [6] D. J. Love, J. Choi, and P. Bidigare, "A closed-loop training approach for massive MIMO beamforming systems," in *Information Sciences and Systems (CISS), 2013 47th Annual Conference on*, 2013, pp. 1-5. [Article \(CrossRef Link\)](#).
- [7] H. Hoon, A. M. Tulino, and G. Caire, "Network MIMO With Linear Zero-Forcing Beamforming: Large System Analysis, Impact of Channel Estimation, and Reduced-Complexity Scheduling," *Information Theory, IEEE Transactions on*, vol. 58, pp. 2911-2934, 2012. [Article \(CrossRef Link\)](#).
- [8] H. Hoon, G. Caire, H. C. Papadopoulos, and S. A. Ramprasad, "Achieving "Massive MIMO" Spectral Efficiency with a Not-so-Large Number of Antennas," *Wireless Communications, IEEE Transactions on*, vol. 11, pp. 3226-3239, 2012. [Article \(CrossRef Link\)](#).
- [9] B. O. Lee, H. Je, O.-S. Shin, and K.-B. Lee, "A novel uplink MIMO transmission scheme in a multicell environment," *Wireless Communications, IEEE Transactions on*, vol. 8, pp. 4981-4987, 2009. [Article \(CrossRef Link\)](#).
- [10] Y. Li, G. Zhu, and S. Zhang, "Transmitter Centric Scheduling in Multi-Cell MIMO Uplink System," in *Communications (ICC), 2010 IEEE International Conference on*, 2010, pp. 1-6. [Article](#)

- [\(CrossRef Link\)](#).
- [11] H. A. David and H. N. Nagaraja, *Order statistics*, 3rd ed.: John Wiley & Sons, Inc., 2004. [Article \(CrossRef Link\)](#).
- [12] A. Rajanna and N. Jindal, "Multiuser Diversity in Downlink Channels: When Does the Feedback Cost Outweigh the Spectral Efficiency Benefit?," *Wireless Communications, IEEE Transactions on*, vol. 11, pp. 408-418, 2012. [Article \(CrossRef Link\)](#).
- [13] O. Somekh, O. Simeone, Y. Bar-Ness, and A. M. Haimovich, "Distributed Multi-Cell Zero-Forcing Beamforming in Cellular Downlink Channels," in *Global Telecommunications Conference, 2006. GLOBECOM '06. IEEE*, 2006, pp. 1-6. [Article \(CrossRef Link\)](#).
- [14] W.-Y. Shin, D. Park, and B. C. Jung, "Can One Achieve Multiuser Diversity in Uplink Multi-Cell Networks?," *Communications, IEEE Transactions on*, vol. 60, pp. 3535-3540, 2012. [Article \(CrossRef Link\)](#).



Yanchun Li received the B.Sc. degrees in Electronics and Information Engineering from Huazhong University of Science and Technology (HUST), China, in 2006. He was graduate intern in the Communication Technology Laboratory of Intel Corp., where he participate research on WiMAX 2, from 2007 to 2008. He was research assitant in Computer Science and Engineering department at Hong Kong University of Science and Technology, where he participate the research on Green Network, from 2010 to 2011. He is currently pursuing his PhD at the Electronics and Information Engineering Department at HUST. His research interests are in the areas of Communication Theory, Information Theory and Signal Processing.



Guangxi Zhu received his B.S. in radio engineering from Huazhong Institute of Technology, China, in 1969. He is the expert of assessment group in Academic Degrees Committee of China State Council for Information and Communication Engineering, co-sponsor and director of Future Mobile Communication FuTURE Project Forum, a Committee for National Technical Standardization. He is a professor and chairman of the academic board of the Department of Electronics and Information Engineering, HUST. His research interests include wireless communication and media signal processing. He has published over 300 papers.



Chen Hua is a associate professor in Wuhan Textile University. Her main research field is Network Communications, include optimization theory and technology, etc. From 2005 to now, her presided more than 3 Hubei natural science fund projects and more than 2 Hubei youth fund projects, published more than 15 papers in the field of network communications.



Minho Jo received his Ph.D. in Dept. of Industrial and Systems Engineering, Lehigh Univ., USA in 1994. He received his BA in Industrial Engineering, Chosun University, S. Korea. He is now Professor of Department of Computer and Information Science at Korea University, Sejong. He is one of founding members of the LCD Division, Samsung Electronics in 1994. He is the Founder and Editor in-Chief of KSII Transactions on Internet and Information Systems. He is an Editor of IEEE Network and an Editor of IEEE Wireless Communications, respectively. He is an Associate Editor of Wiley's Security and Communication Networks and an Associate Editor of Wiley's Wireless Communications and Mobile Computing, respectively. He has published many refereed academic publications in very high quality journals and magazines. He is now the Vice President of the Institute of Electronics and Information Engineers. Areas of his current interest include cognitive radio, network algorithms, optimization and probability in networks, network security, wireless communications and mobile computing in 5G and 6G, wireless body area network (WBAN), and wireless organ network (WON).



Yingzhuang Liu is a professor of Huazhong University of Science and Technology (HUST). His main research field is broadband wireless communication, including LTE and IMT Advanced system, etc., especially its Radio Resource Management. From 2000 to 2001, he was a postdoctoral researcher in Paris University XI. From 2003 up to now, he has presided over 10 national key projects, published more than 80 papers and held more than 30 patents in the field of broadband wireless communication. He is now the group leader of broadband wireless research of HUST, which has more than 10 young teachers and more than 20 PhD students.